NANO
LETTERS

XXXX
Vol. xx, No. x
-

Vertically Aligned Nanowires from Boron-Doped Diamond

Nianjun Yang,*,† Hiroshi Uetsuka,† Eiji Osawa,‡ and Christoph E. Nebel§

Diamond Research Center, National Institute of Advanced Industrial Science and Technology (AIST), Tsukuba 305-8568, Japan, NanoCarbon Research Institute, Faculty of Textile Science and Technology, Shinshu University, Nagano 386-8567, Japan, and Fraunhofer Institute of Applied Solid State Physics (IAF), Freiburg 79108, Germany

Received April 21, 2008; Revised Manuscript Received June 13, 2008

ABSTRACT

Vertically aligned diamond nanowires with controlled geometrical properties like length and distance between wires were fabricated by use of nanodiamond particles as a hard mask and by use of reactive ion etching. The surface structure, electronic properties, and electrochemical functionalization of diamond nanowires were characterized by atomic force microscopy (AFM) and scanning tunneling microscopy (STM) as well as electrochemical techniques. AFM and STM experiments show that diamond nanowire etched for 10 s have wire-typed structures with 3−10 nm in length and with typically 11 nm spacing in between. The electrode active area of diamond nanowires is enhanced by a factor of 2. The functionalization of nanowire tips with nitrophenyl molecules is characterized by STM on clean and on nitrophenyl molecule-modified diamond nanowires. Tip-modified diamond nanowires are promising with respect to biosensor applications where controlled biomolecule bonding is required to improve chemical stability and sensing significantly.

Nanowires are new materials, which have characteristics of low weight with sometimes extraordinary mechanical, electrical, thermal, and multifunctional properties.[1,2] By creating these nanostructures, it is possible to control the fundamental properties of materials without changing their chemical composition. Nanowire-based substrates can be used for tunable transport of electrons with electronic properties strongly influenced by little perturbations on the surface and for giant surface-to-volume ratio enhancements. In this way the attractive world of low dimensional systems, together with the fabrication of functional nanostructured arrays are important for chemical/biochemical applications, and for a generation of well-defined molecular patterns on biosensor surfaces. These nanowires thus will play a major role in the new trend of chemical and biochemical nanotechnology.[1,2]

Nanowires are generated by (a) self-assembly of small-sized structures to form larger structures ("bottom up") or (b) by reduction of large systems down to small size ("top-down"), which have been applied on materials like Si,[3] gold,[4] glassy carbon,[5] SnO_2,[6] and ZnO_2.[7] However, they do not possess the desired chemical stability and reproducibility of surfaces in electrolyte solutions. Only diamond is known to be outstanding with respect to electrochemical properties[8−10] due to low background current, wide working window, and good chemical stability even in solutions. The surface of diamond shows unique properties as it can be terminated with hydrogen, with oxygen, and with OH, which allows optimizing the electronic properties of the solid/electrolyte interface.[11−13] In addition, diamond shows strongest bonding stability to DNA and thus has been widely utilized for biosensor applications recently.[14] Diamond is ultrahard (50−150 GaP) which is promising with respect to mechanical stability of diamond nanowires.[15]

The realization of diamond nanowires started already in 1997 by Shiomi,[16] who demonstrated for the formation of porous diamond films by reactive ion etching (RIE) using O_2. Later in 2000, nanostructured diamond honeycomb films have been prepared[17] by etching through a porous anodic alumina mask, triggering some activities which are summarized in an article of Shenderova et al.[18] Growth-induced formation of nanoscale tubular structures have been reported for the first time in 2003, applying a microwave plasma of hydrogen under a bias potential.[19] In 2008, Zou et al.[20] reported about the fabrication of nanopilar arrays using self-aligned Au nanodots as etching mask in a bias-assisted reactive ion etching, applying a hydrogen/argon plasma. Although these achievements demonstrate that vertically aligned diamond nanowires can be fabricated by a variety of methods, no applications in electro- or biochemistry have been reported up to now.

* To whom correspondence should be addressed. E-mail: nianjun-yang@asit.go.jp.
† National Institute of Advanced Industrial Science and Technology (AIST).
‡ Shinshu University.
§ Fraunhofer Institute of Applied Solid State Physics (IAF).

10.1021/nl801136h CCC: $40.75
Published on Web 09/23/2008

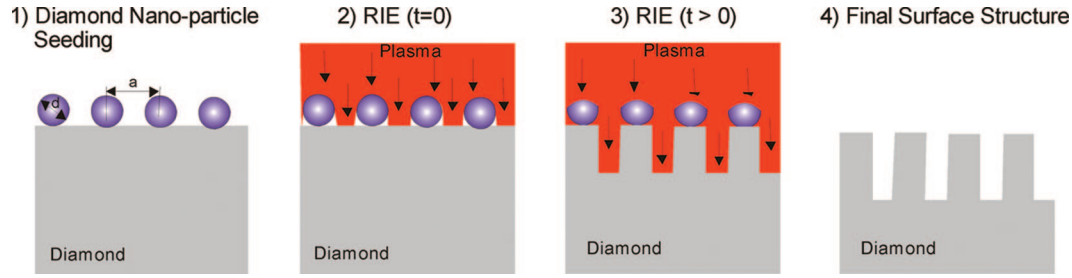

Figure 1. Schematic plots of fabrication of diamond nanowires. Here *d* is the diameter of nanodiamond particles, and *a* is the distance between particles. RIE denotes reactive ion etching. Refer to the text to obtain the details.

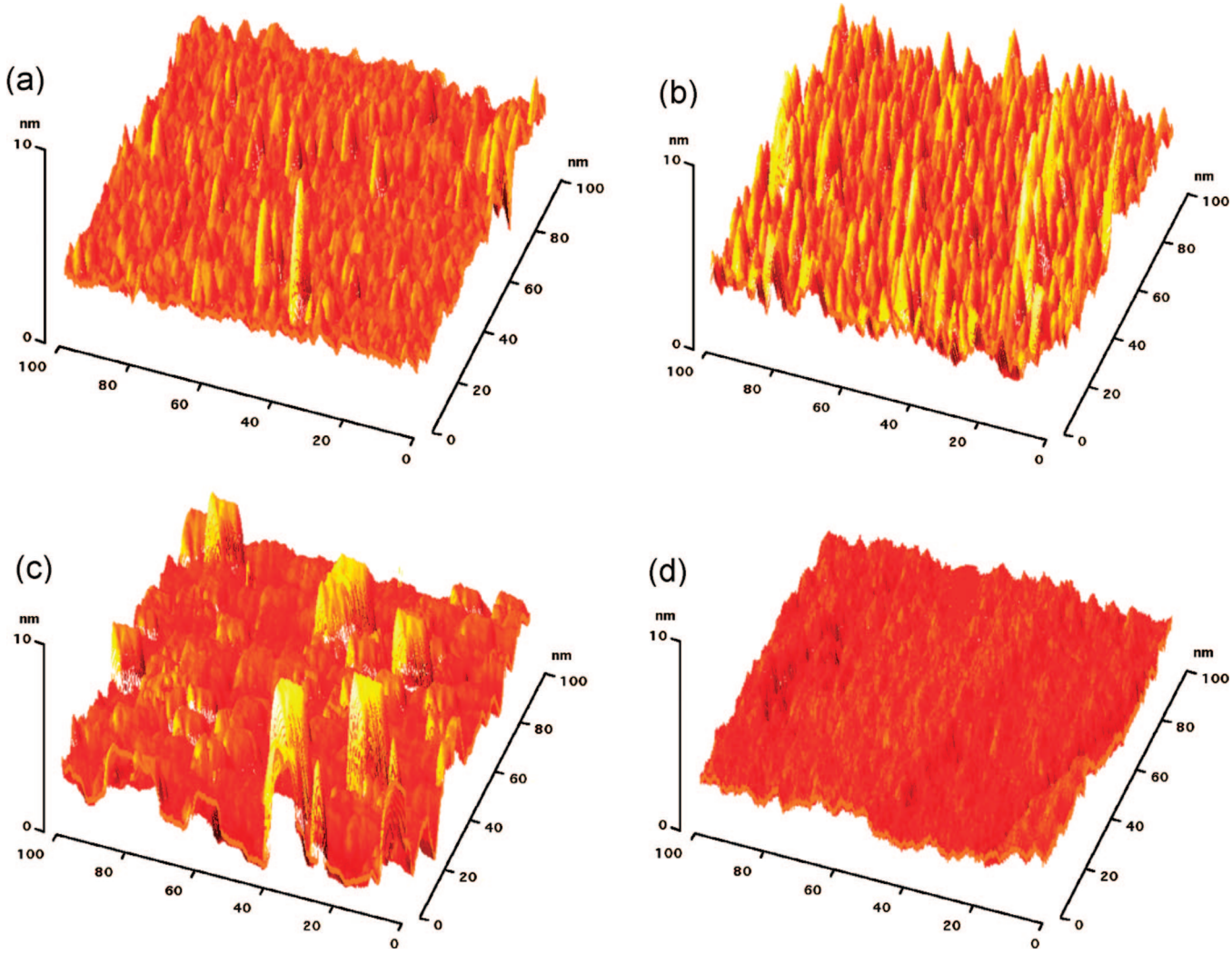

Figure 2. AFM images of diamond surface after RIE-etching with a gas mixture of 3% CF_4 and 97% O_2 for an etching time of (a) 5, (b) 10, (c) 20, and (d) 60 s.

In this paper, we introduce for the first time the fabrication of vertically aligned diamond nanowires from a metallically boron-doped single crystalline CVD diamond by use of a top-down procedure, as schematically shown in Figure 1. First, metallically boron-doped (p-type) diamonds with atomically smooth surfaces are grown by homoepitaxy on Ib diamond substrates, using a microwave-assisted chemical vapor deposition technique.[21] The root-mean-square (rms) roughness of the surface is typically about 0.8 Å. Then, an etching mask from diamond nanoparticles is deposited. Diamond nanoparticles, as shown in Figure 1, can be produced with well-defined size and quality.[22] We have applied here diamond nanoparticles of typical 8−10 nm in diameter. These particles are dissolved in water by ultrasonification (200 W, 20 kHz, 12 h) to form a pseudostable suspension.[22−24] The concentration of this suspension is crucial and pretreatment of diamond powder affects the stability of the suspension. Then the diamond plate is immersed into the suspension and sonificated (100 W, 10 min) to seed diamond nanoparticles on the diamond surface. The diamond nanoparticle layer is dense and depends on suspension quality and time of sonification. After deposition

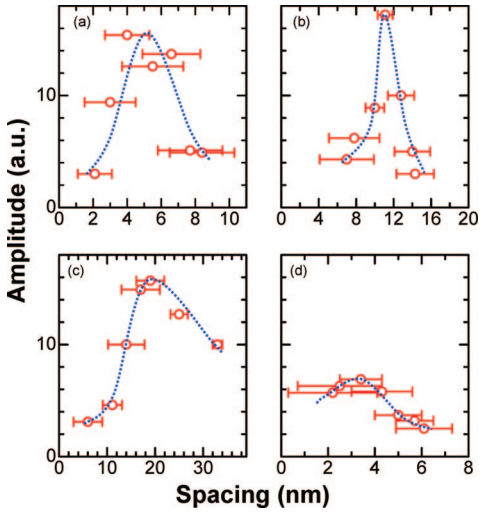

Figure 3. Surface analysis of nanowires fabricated for an etching time of (a) 5, (b) 10, (c) 20, and (d) 60 s.

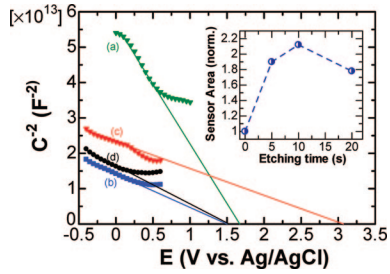

Figure 4. Mott−Schottky plots of a smooth diamond (a) and diamond nanowires for an etching time of (b) 5, (c) 10, and (d) 20 s in 0.1 M pH 7.4 phosphate buffer at a fixed frequency of 1.0 kHz. The inset is the sensor area calculated as a function of etching time.

of nanoparticles, reactive ion etching (RIE) in an O_2 (97%)/CF_4 (3%) gas mixture is applied for typical times between 2 to 60 s. The diamond etching rate is 10 Å s^{-1}. Vertically aligned diamond nanowires arise where diamond nanoparticles have been deposited. They act as an etching mask as shown schematically in Figure 1. Detailed geometrical properties of wires depend on the size and etching rate of nanoparticles. The length of wires can be up to several micrometers if, for example, silicon instead of diamond particles is used as silicon is more resistant against etching (etching rate 1 Å s^{-1}).

Figure 2 shows four AFM tapping mode images of diamond after RIE etching for 5, 10, 20, and 60 s, using diamond nanoparticles as hard mask. Each of these surfaces has been evaluated using Fourier-analysis to determine the geometrical properties. The results of these calculations are shown in Figure 3. Etching for 5 s (Figures 2a and 3a) generates short wires of less than 20 Å in length. The average distance between wires is in the range of 5 nm, varying from 2 to 9 nm. An etching for 10 s (Figurse 2b and 3b) results in wires with diameters of 1 to 5 nm. They are distributed regularly on the surface with about 11 nm distance in between wires. Etching for longer times results in deterioration of these properties as can be seen in Figures 2c,d and 3c,d. After 20 s etching, the wires become undefined, varying

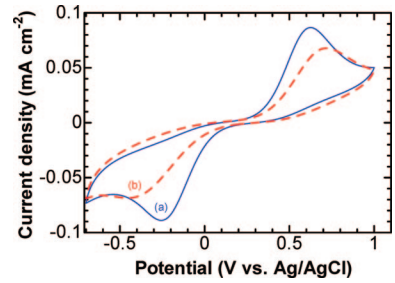

Figure 5. Cyclic voltammograms of 1.0 mM $Fe(CN)_6^{3-/4-}$ at a scan rate of 0.1 V s^{-1} in pH 7.4 phosphate buffer on diamond nanowires before (a) and after (b) nitrophenyl attachment.

in shape, height, and periodicity. Finally, after 60 s etching the wire structure vanishes and a relative smooth surface is generated.

Vertically aligned diamond nanowires with optimized geometrical dimensions of 10 nm length and an average separation of 11 nm were obtained with an etching time of 10 s. As the etching rate of diamond nanoparticles is about 10 Å s^{-1}, 10 s is the time these particles act as an etching mask. It demonstrates that geometrical properties of self-aligned particles rule the formation of vertically aligned diamond nanowires.

To evaluate the interfacial electronic properties of diamond nanowires to phosphate buffer of pH 7.4, we have performed capacitance (C)−voltage (V) measurements at 1 kHz. The results are shown in Figure 4 as Mott−Schottky plot (C^{-2} as a function of potential). We use the Mott−Schottky equation to calculate the built-in potential and the variation of sensors area, given by

$$\frac{1}{C^2} = \frac{2}{\varepsilon_0 \varepsilon_r A^2 N_B}\left(V - V_{bi} - \frac{kT}{e}\right)$$

where ε_0 is the dielectric constant, $\varepsilon_r = 5.7$ (diamond), A is the active sensor area, N_B the boron acceptor density in diamond, V_{bi} the built-in potential, k the Boltzmann constant, T the temperature (300 K), and e the elementary charge. In these experiments, the acceptor concentration was fixed (N_B = constant) as parts of the same diamond have been used. If N_B is constant, variations of slope arise from variations in active area.

Smooth diamond shows a doping concentration of 7×10^{19} cm^{-3} and a built-in potential of 1.6 V, as the surface is hydrogen terminated. The depletion layer width at the interface is about 10 Å. After etching for 5, 10, and 20 s the Mott−Schottky graphs are changing significantly. The active sensor area is increasing by RIE, showing a maximum of $2.1 \times A_0$ after 10 s RIE, where A_0 is the smooth surface area. This is shown in the inset of Figure 4. The built-in potential is changing as hydrogen is removed from the surface and surface defects give rise to surface Fermi-level pinning. It is interesting, that the highest barrier of 3.1 eV is generated by 10 s RIE, while shorter (5 s) or longer (20 s) etching times do not change the built-in potential.

These nanowires for an etching time of 10 s are functionalized by use of an electrochemical phenyl-linker molecule attachment schema,[25−27] which preferentially bonds phenyl linker-molecules to tips of wires, because on structured

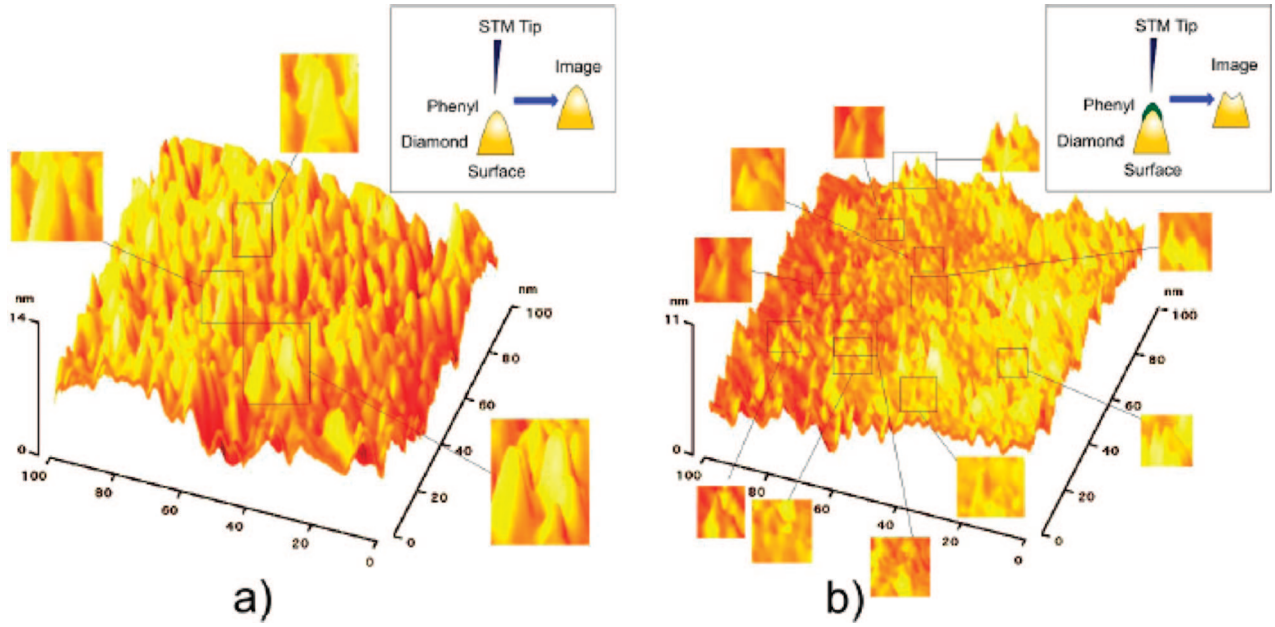

Figure 6. STM images of diamond nanowires (a) before and (b) after the electrochemical grafting of a nitrophenyl film by a constant potential technique at −0.05 V vs Ag/Ag^+ for 4 s.

surfaces like vertically aligned nanowires the electric field concentrates at tips of wires, which stimulates current flow preferentially through wires and their tips. To investigate well-defined nitrophenyl bonding to wire tips we have performed attachment experiments using constant potential attachment with −0.05 V (versus Ag/Ag^+) for 4 s. The attachment potential has been selected from cyclic voltammetric attachment experiments, performed to detect the reduction peak potential on oxidized and RIE-etched diamond surfaces which are shifted to this lower potential.

The electrochemical properties of vertically aligned diamond nanowires before and after nitrophenyl attachments were examined by use of the redox couple of $Fe(CN)_6^{3-/4-}$ as mediators. Figure 5 shows the variation of $Fe(CN)_6^{3-/4-}$ redox currents by phenyl attachment. Diamond nanowires before attachment have oxidized surface properties which give rise to a peak splitting of 868 mV between anodic and cathodic peak. This wide potential separation is also a result of the relative low doping concentration of diamond of only 7×10^{19} cm^{-3}. After phenyl attachment, the redox peak currents decrease by about 22% and shift even wider in potential with 1160 mV peak separation. However, the surface is still redox active.

Moreover, nitro- to amino-phenyl conversions were detected on such modified nanowire electrodes.[25−27] Here, four cyclic scans have been applied to convert nitro- to amino-phenyl. Please note that on smooth diamond surfaces only one scan is required.[25−27] The origin of this is currently under investigation.

In order to identify locations of nitrophenyl attachment to diamond nanowires, constant-current mode STM has been employed to image the diamond nanowires before and after grafting with nitrophenyl. Sharp tips of 3−10 nm size and 8−10 nm length are detected in the clean diamond nanowires (Figure 6a). This result agrees with AFM data shown in Figure 2b; STM on phenyl-modified wires shows a drastic change of tip features. A "double peak" structure is detected, which is a result of constant tunneling current mode applied here. As nitrophenyl films are insulating, they give rise to decreased STM tunneling currents. To keep the tunneling current constant, the STM tip will approach toward the surface which results in inverted cone-shaped tips as shown in Figure 6b. From these data we conclude that electrochemical modifications of vertically aligned diamond nanowires give rise to phenyl bonding to the tips of wires while in between most of the surface remains uncoated.

These electrochemically functionalized diamond nanowires have been applied for DNA sensing. The goal is to combine the outstanding electrochemical properties of diamond (e.g., good chemical stability, low background current, wide potential window, ultra hardness) with the advantage of geometrically controlled bonding of DNA molecules to the nanostructured transducer to achieve a "like-in-solution" situation."[28]

In summary, nanodiamond particles dispersed on a smooth diamond electrode can be utilized as an etching mask for the fabrication of vertically aligned diamond nanowires with controlled length and nanoscaled spacing between wires. Tips of nanowires can be functionalized electrochemically as a result of electric field concentration at the tips of wires. Please note that for these experiments, the doping of diamond was in the range of 7×10^{19} cm^{-3}, which is nearly a factor of 10 below the doping density conventionally applied. It gives rise to huge redox current peak splitting, but nonetheless these experiments clearly show the major properties that come by fabrication of vertically aligned diamond nanowires. For applications as gas sensors, we expect that for even lower doping levels for biosensor applications the doping level needs to be significantly enhanced. Control of geometrical properties of nanowires is promising for the realization of

biosensors which require controlled mesospacing of molecules like DNA or enzymes on transducer surfaces to improve sensing properties significantly. The applications of such functionalized diamond nanowires for DNA sensing are currently performing in our laboratory and will be introduced in the near future.

Acknowledgment. The authors want to thank Dr. O. Williams (Institute for Materials Research, Hasselt University, Belgium) for helping establish the seeding of diamond nanoparticles on diamond surface as a JSPS visiting scientist in our laboratory.

References

(1) Zheng, G.; Patolsky, F.; Cui, Y.; Wang, W. U.; Lieber, C. M. *Nat. Biotechnol.* **2005**, *23*, 1294–1301.
(2) Cui, Y.; Wei, Q. W.; Park, H.; Lieber, C. M. *Science* **2001**, *293*, 1289–1292.
(3) Strother, T.; Cai, W.; Zhao, X. S.; Hamers, R. J.; Smith, L. M. *J. Am. Chem. Soc.* **2000**, *122*, 1205–1209.
(4) Hashimoto, K.; Ito, K.; Ishimori, Y. *Anal. Chem.* **1994**, *66*, 3830–3833.
(5) Millan, K. M.; Spurmanis, A. J.; Mikkelsen, S. R. *Electroanalysis* **1992**, *4*, 929–932.
(6) Yusta, F. J.; Hitchman, M. L.; Shamlian, S. H. *J. Mat. Chem.* **1997**, *7*, 1421–1427.
(7) Elrehim, S. S. A.; Elwahab, S. M. A.; Fouad, E. E.; Hassan, H. H. *Mater. Corros.* **1995**, *46*, 633–638.
(8) Angus, J. C.; Pleskov, Y. V.; Eaton, S. C. Electrochemistry of diamond. In *Thin Film Diamond II, Semiconductors and Semimetals*; Nebel, C. E., Ristein, J., Eds.; Elsevier Academic Press: New York, 2004; Vol. 77, p 97.
(9) Swain, G. M. Electroanalytical applications of diamond electrodes. In *Thin Film Diamond II, Semiconductors and Semimetals*; Nebel, C. E., Ristein, J., Eds.; Elsevier Academic Press: New York, 2004; Vol. 77, p 121.
(10) Nebel, C. E.; Rezek, B.; Shin, D.; Uetsuka, H.; Yang, N. *J. Phys. D: Appl. Phys.* **2007**, *40*, 6443–6466.
(11) Cui, J. B.; Ristein, J.; Ley, L. *Phys. Rev. Lett.* **1998**, *81*, 429–432.
(12) Ristein, J.; Riedel, M.; Ley, L. *J. Electrochem. Soc.* **2004**, *151*, E315–E321.
(13) Nebel, C. E. *Science* **2007**, *318*, 1391–1392.
(14) Yang, W.; Auciello, O.; Butler, J. E.; Cai, W.; Carlisle, J. A.; Gerbi, J. E.; Gruen, D. M.; Knickerbocker, T.; Lasseter, T. L.; Russell, J. N., Jr.; Smith, L. M.; Hamers, R. J. *Nat. Mater.* **2007**, *1*, 253–257.
(15) Blank, V.; Popov, M.; Pivovarov, G.; Lvova, N.; Gogolinsky, K.; Reshetov, V. *Diamond Relat. Mater.* **1998**, *7*, 427–431.
(16) Shiomi, H. *Jpn. J. Appl. Phys.* **1997**, *36*, 7745–7748.
(17) Masuda, H.; Watanabe, M.; Yasui, K.; Tryk, D.; Rao, T.; Fujishima, A. *Adv. Mater.* **2000**, *12*, 444–447.
(18) Shenderiva, O. A.; Padgett, C. W.; Hu, Z.; Brenner, D. W. *J. Vac. Sci. Technol., B* **2005**, *23*, 2457–2464.
(19) Kobashi, K.; Tachibana, T.; Yokota, Y.; Kawakami, N.; Hayashi, K.; Yamamoto, K.; Koga, Y.; Fujiwara, S.; Gotoh, Y.; Nakahara, H.; Tsuji, H.; Ishikawa, J.; Köck, F. A.; Nemanich, R. J. *J. Mat. Res.* **2003**, *18*, 305–326.
(20) Zou, Y. S.; Yang, Y.; Zhang, W. J.; Chong, Y. M.; He, B.; Bello, I.; Lee, S. T. *Appl. Phys. Lett.* **2008**, *92*, 053105. (1−3).
(21) Tokuda, N.; Umezawa, H.; Saito, T.; Yamabe, K.; Okushi, H.; Yamasaki, S. *Diamond Relat. Mater.* **2007**, *16*, 767–770.
(22) Kruger, A.; Kataoka, F.; Ozawa, M.; Fujino, T.; Suzuki, Y.; Aleksenskii, A. E.; Vul, A. Y.; Osawa, E. *Carbon* **2005**, *43*, 1722–1730.
(23) Williams, O. A.; Douheret, O.; Daenen, M.; Haenen, K.; Osawa, E.; Takahashi, M. *Chem. Phys. Lett.* **2007**, *445*, 255–258.
(24) Williams, O. A.; Daenen, M.; DHaen, J.; Haenen, K.; Maes, J.; Moshchalkov, V. V.; Nesladek, M.; Gruen, D. M. *Diamond Relat. Mater.* **2006**, *15*, 654–658.
(25) Uetsuka, H.; Shin, D.; Tokuda, N.; Saeki, K.; Nebel, C. E. *Langmuir* **2007**, *23*, 3466–3472.
(26) Shin, D.; Tokuda, N.; Rezek, B.; Nebel, C. E. *Electrochem. Commun.* **2006**, *5*, 844–850.
(27) Rezek, B.; Shin, D.; Nakamura, T.; Nebel, C. E. *J. Am. Chem. Soc.* **2006**, *128*, 3884–3885.
(28) Yang, N.; Uetsuka, H.; Osawa, E.; Nebel, C. E. *Angew. Chem.* **2008**, *120*, 5261–5263; *Angew. Chem., Int. Ed.*, **2008**, *47*, 5183–5185.

NL801136H